

The effect of contact stress on the sliding wear behaviour of Zn-Ni electrodeposited coatings

L. Lee, P. Behera, K. R. Sriraman & R. R. Chromik*

Department of Mining & Materials Engineering, McGill University, Montreal, Qc, Canada

* Corresponding author email: richard.chromik@mcgill.ca

Abstract

Zinc-Nickel coatings, developed in the 1980's as a replacement for zinc coatings in the automotive industry, have recently gained interest in the aerospace industry to replace cadmium coatings. Due to different material properties of Zn-Ni and Cd, there is a need to characterize Zn-Ni for tribological applications. Sliding wear tests are performed on a reciprocating pin-on-flat tribometer using a steel counterface on two Zn-Ni coatings with different microstructure and surface topography. Tests were performed under 3, 7.5 and 12 N normal loads at a relative humidity of 60 % for 2000 cycles. Increasing the normal load increased the steady state friction coefficient and wear for both coatings. The smooth and dense coating was more sensitive to the change in normal load than the rough and porous coating, as the latter experienced less wear due to the columnar structure of the coating. In contrast, the smoother and dense coating, although has less wear at low loads, has more wear at high loads due to debonding of the coating. So the coating morphology affected the extent of wear due to different wear and velocity accommodation mechanisms.

Keywords: Sliding wear; surface topography; intermetallic alloy; wear

1. Introduction

Zinc-Nickel alloy coatings were developed in the 1980's as a corrosion protective coating for the automotive industry [1]. Recently, they have attracted attention from the aerospace industry as a replacement for cadmium, which is used as a corrosion protection coating for steel, but is toxic, carcinogenic and some cadmium plating baths contain cyanide [2-7]. Cadmium is used in the aerospace industry on landing gear components and fasteners, where both corrosion and tribological properties are important. Zn-Ni coatings, being a well-utilized corrosion resistant coating for more than three decades, are a leading candidate to replace Cd coatings. However, while many studies have been made on the corrosion properties of Zn-Ni coatings [1, 4, 5, 8-13], fewer studies have been made on the tribological properties of Zn-Ni coatings [3, 10, 14-16].

Recent studies on the tribology of Zn-Ni coatings include works by Sriraman *et al.* [3, 10], where the sliding wear and tribocorrosion properties of Zn-Ni and Cd were compared. They found that Zn-Ni has a better wear and corrosion resistance during sliding wear and sliding wear tests performed in 3.5 % NaCl solution. Panagopoulos *et al.* [16] conducted tribology tests on Zn-Ni and found a higher but more stable coefficient of friction (CoF) for alumina counterfaces compared to steel. Increasing the load lowered the CoF but an increase in wear was observed for both cases. Ghaziof and Gao [14] studied the effects of plating parameters on the Ni content, morphology and wear resistance of Zn-Ni coatings. They found that coatings which contained γ -ZnNi with a smoother nodular morphology and higher hardness exhibited better wear resistance and a lower COF than mixed η and γ -phases coatings with cauliflower-like morphology and/or γ -phase coatings with larger and coarser nodular structure.

Varying the plating conditions will vary the morphology of the coating, which is one of the main differences between commercially available Zn-Ni coatings [14]. Surface morphology has an important role on the tribological properties of a system. Effects of surface morphology have been studied previously with many bulk materials and can have a strong effect on the friction and wear behaviour, especially during the initial run-in period [17]. Surface morphology and roughness have a strong effect on the initial contact area, where a higher surface roughness results in a lower contact area. Minimizing the contact area minimizes adhesion, friction and wear [18]. Although higher surface roughness minimizes the contact area, studies have correlated greater wear with higher roughness [17, 19, 20]. Therefore, differences in the surface morphology can affect the friction and wear behaviour of the system.

Trends of friction and wear with roughness may be modified by changing the contact conditions, such as the normal load [16, 20-24]. Dependence of friction to the normal load in unlubricated metal-metal contacts varies with the system. In instances where the friction and wear were high, such as the case of steel-aluminum contact, the

normal load did not significantly influence the friction [24]. In contrast, in metal contacts which forms an oxide layer, such as copper-copper contacts, a low CoF was observed at lower loads due to the lubricating properties of the oxide layer, whereas at higher loads, the oxide layer was broken down, and a high CoF was observed [24]. In some instances, when an increase in load was coupled with a rougher surface or wear debris, a decrease in CoF was observed [24]. In the case of Zn-Ni, Panagopoulos *et al.* [16] found that only at the highest load used resulted in a decreased steady state friction, whereas at lower loads, there was no significant change in the steady state friction.

Tribological studies of Zn-Ni alloy coatings are sparse in the open literature and important aspects, such as surface morphology and loading effects, need to be understood for successful implementation of these coatings in new settings that require good tribological performance. Here, we studied two commercially available Zn-Ni coating with distinctly different surface morphology. The sliding friction and wear behaviour of the coatings were studied by varying the load using a pin-on-flat reciprocating tribometer. Correlations of the surface morphology with the loading conditions are made through *ex situ* examination of the worn surfaces and transfer films.

2. Methods

2.1 Coating Process

Two commercially available zinc-nickel coatings were plated in industrial pilot plating tanks. The Zn-Ni alloy coating was deposited onto 100 x 160 x 0.8 mm³ low carbon steel sheets (SAE 1006).

C-ZnNi coatings were plated using an alkaline NaOH (120-135 g/L) based plating solution containing 7-10 g/L zinc and 1-1.8 g/L nickel. Plating was performed at 21-25 °C temperature and 10 mA/cm² current density. Plated samples were then passivated using a blue trivalent chrome passivate and baked at 200°C for 24 hours. [25, 26]

D-ZnNi coatings were plated using an alkaline NaOH (135 g/L) based plating solution with the Zn:Ni ratio maintained at 10-11:1 and the pH maintained at 12-13.5. Plating was performed at 25 °C temperature and 50 mA/cm² current density. Prior to plating, substrates were grit blasted and acid pickled with HCl. Plated samples were then passivated with a blue trivalent conversion coating and baked at 200°C for 24 hours. [8]

2.2 Characterization

Scanning electron microscopy (SEM) was used to observe the as-received coatings, wear tracks and transfer films. An FEI Inspect F-50 microscope (US) with a field emission source was used. Selected specimens were observed in cross section, which

were cut with a diamond blade, mounted in conductive epoxy, grounded with SiC paper and polished using a 10% mixture of alumina and propanol.

X-ray diffraction (XRD) was used to confirm the phases present in both coatings and measure residual stress. A Bruker Discover D8-2D (US) with a Cu-K α source was used in the standard θ -2 θ mode on the as-received coatings. Biaxial residual stresses on the lateral and longitudinal directions of the coatings were measured on the peak corresponding to the (721) miller index using a standard $2\theta \sin^2\psi$ method [27].

Adhesion of the coating to the substrate was characterized using a microscratch tester by CSM Instruments (Switzerland) with a 200 μm Rockwell C diamond tip. Incremental load scratch tests from 0 N to 30 N with a scratch length of 5 mm were performed at a rate of 5 mm/min.

Profilometry was performed using a white light profilometer (Wyko NT8000, Veeco, US) on the as-received coating to obtain the initial coating roughness and profiles of the wear tracks used to calculate wear rate. Wear volumes of the wear tracks were calculated based on the average wear area and multiplied by the wear track length. Ten profiles were made along the wear track and used to calculate the average wear area. The average wear area is determined by material loss below the average surface line and calculated by integrating the area below the surface. The wear rate was calculated using the Archard and Hirst equation [28] shown in Equation 1.

$$K = \frac{\text{Volume of wear}}{(\text{Normal Load}) \times (\text{Distance})}, \quad (\text{Eq 1})$$

Chemical analyses of the oxide phases on the tribofilm were performed using Raman spectroscopy (inVia Raman microscope by Renishaw, UK) which has a 514.5 nm Ar⁺ laser excitation source. A laser power of 2.5 mW is used.

Electron probe micro analyzer (EPMA) test was previously performed in [15] to assess the composition of the coatings and C-ZnNi contained 14.63 ± 0.05 wt.% Ni while D-ZnNi contained 15.65 ± 0.58 wt.% Ni. Mechanical properties of the coatings were also previously performed in [15] and similar reduced moduli of $E_r = 127 \pm 15$ GPa for C-ZnNi and 137 ± 12 GPa for D-ZnNi were found. Hardness of the coatings differ (C-ZnNi: $H = 5.2 \pm 0.3$ GPa, D-ZnNi: $H = 6.6 \pm 0.3$ GPa), and may be attributed to the differences in Ni content and crystallographic orientation.

2.3 Wear Test

Wear tests were performed using a reciprocating pin-on-flat tribometer using 6.35 mm diameter AISI 440C steel ball counterfaces. The relative humidity and

temperature were kept at 60% and 20-25°C, respectively. A sliding speed of 14 mm/s was used. The normal loads of 3.5, 7 and 12 N were used to evaluate the effect of initial Hertzian contact stress (IHCS) on the wear behaviour of the coating. Using a Young's Modulus of 118 GPa and Poisson's ratio of 0.23 for Zn-Ni [29, 30], these normal loads correspond to an estimated maximum IHCS of 750, 940, 1130 MPa, respectively when considering a contact with no roughness. Stripe tests were performed on these coatings, where an initial track length of 20 mm was decreased by 2 mm at cycles 10, 75, 200, 500 and 850, while the sliding speed remains constant. A total of 2000 cycles were performed, amounting to a total sliding distance of 46.54 m.

3. Results

3.1 Characterization

The surface of C-ZnNi coatings shows a smooth coating formed through fine platelet agglomerations (Figure 1a). Cross section of the coatings reveals a dense coating with through thickness vertical cracks and small porosities (Figure 1b). The surface of D-ZnNi coating shows platelets agglomerated into hemispherical shapes, resulting in a rough coating with through coating porosity (Figure 1c). Cross section of the coating shows cracks along the agglomerates and small porosities (Figure 1d). Profilometry results shows a higher roughness for the D-ZnNi coating ($R_a = 2.90 \pm 0.35 \mu\text{m}$) than C-ZnNi coating ($R_a = 1.35 \pm 0.19 \mu\text{m}$) [15]. Both as received coatings are γ -ZnNi phase and the XRD results are presented in Figure 2. Biaxial residual stress measurements on the coatings show tensile stresses for C-ZnNi and compressive stresses for D-ZnNi.

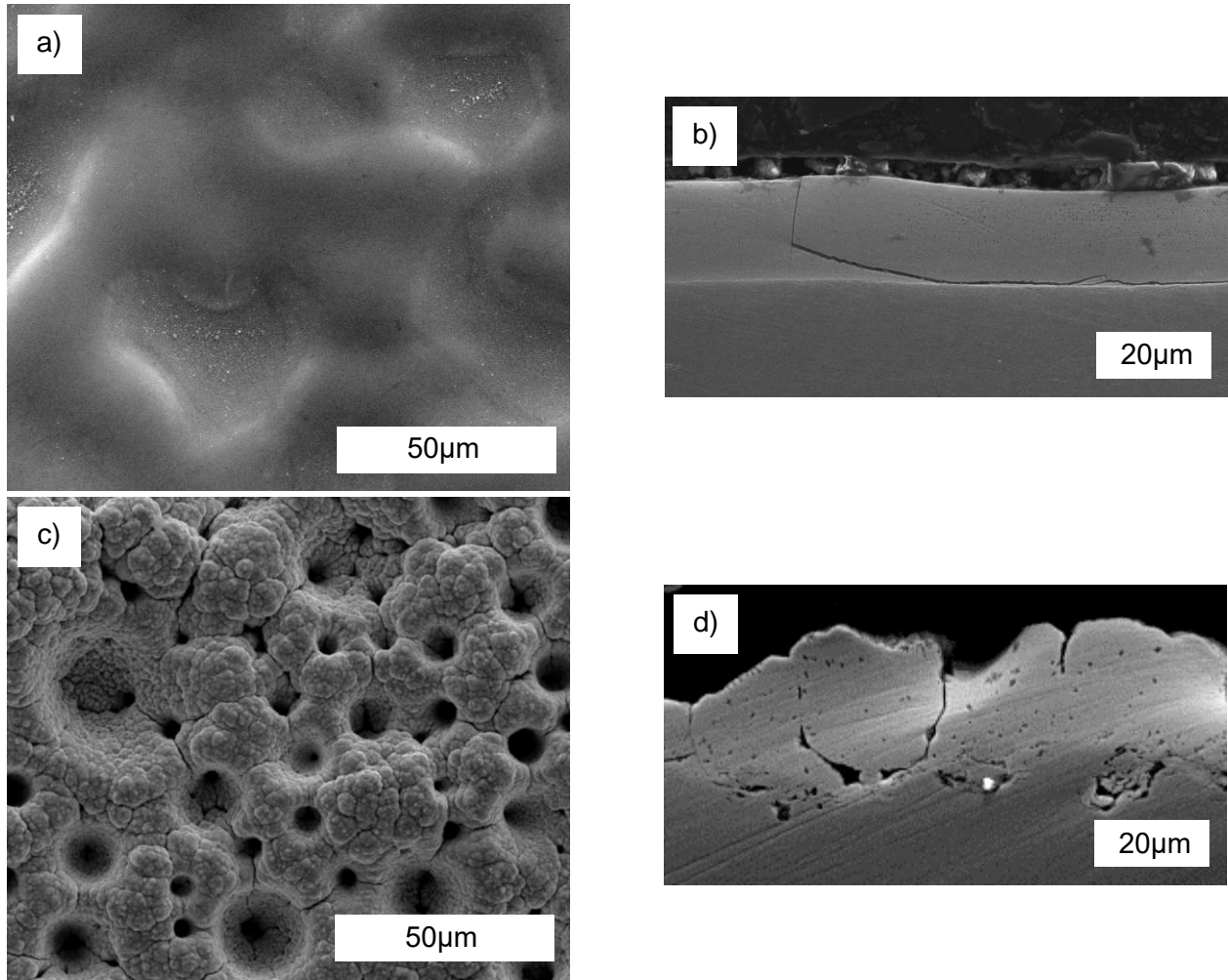


Figure 1. C-ZnNi a) surface morphology and b) cross section, and D-ZnNi c) surface morphology and d) cross section secondary electron images [15]

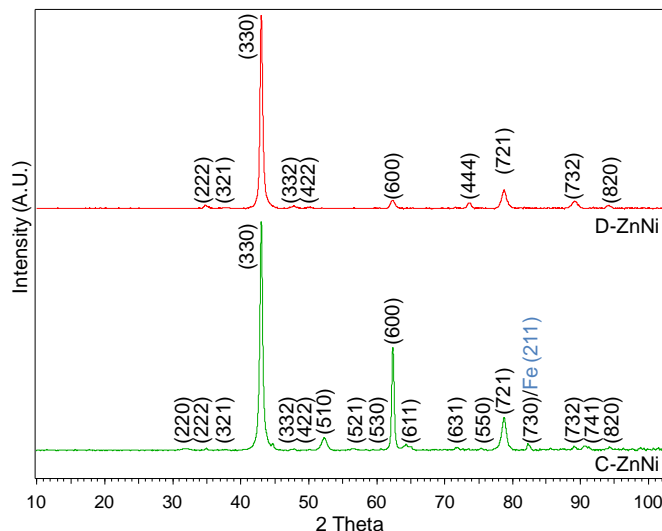


Figure 2. XRD diffraction pattern of C-ZnNi and D-ZnNi coatings, peaks corresponding to γ -ZnNi

3.2 Scratch testing

Scratch testing was performed on the coatings to test the adhesion of the two coatings to the substrates and are shown in Figure 3. Both coatings showed good adhesion to the substrate. No decohesion at the interface is observed. Ductile failure modes through tensile cracking are observed for both coatings at the beginning of the scratch test, and near the end of the test, the coating is scraped off due to coating thickness and the steel substrate is exposed [31, 32]. However, for C-ZnNi coatings, cracks are observed at the onset of the scratch and continued through the scratch as cracks and spallation at the sides of the track. Cracking and spallation at the sides of the track are not observed in tests performed on D-ZnNi coating. In addition, the scratch is accommodated by D-ZnNi coatings through deformation of the plating agglomerates, as the coating porosity is closed. The onset of tensile cracks (indicated by the number 1) also occurred earlier in the tests for C-ZnNi coatings. The onset of continuous exposure (indicated by the number 2) also occurred earlier for C-ZnNi coatings. Also, for C-ZnNi coatings, patches of steel are exposed as the coating is removed (indicated by number 3), which corresponds to a discontinuity observed in the tangential force. The width of the scratch tracks is also wider for C-ZnNi coatings than D-ZnNi coatings. The difference in the width of the scratch tracks can be correlated to the hardness, as D-ZnNi is harder than C-ZnNi a wider track is expected for C-ZnNi.

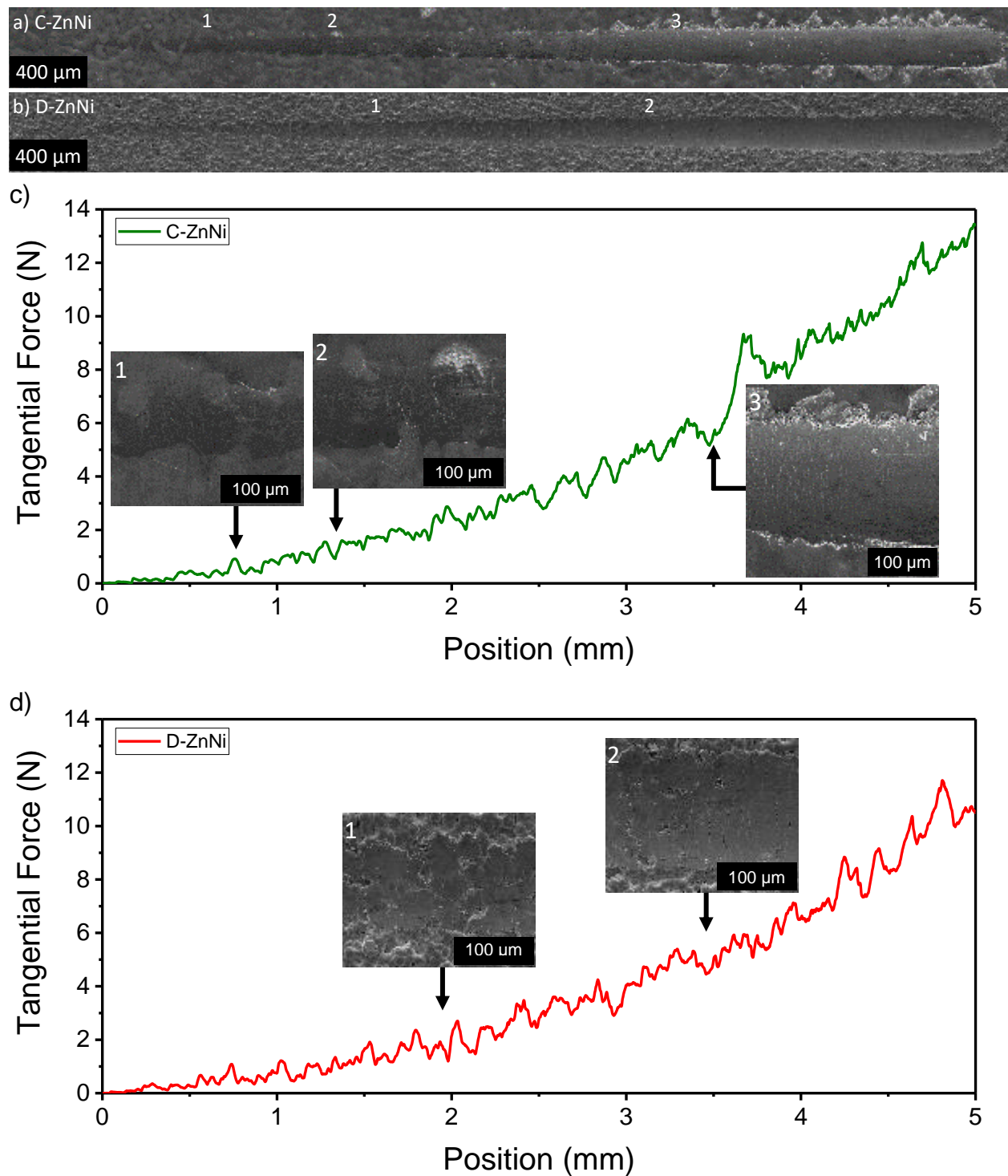


Figure 3. Optical images of scratch test performed on a) C-ZnNi and b) D-ZnNi coatings and corresponding tangential forces for c) C-ZnNi and d) D-ZnNi, with numbers indicating transitions

3.3 Wear Test

Sliding wear tests were performed on the two different coatings. Figure 4 shows the evolution of coefficient of friction (CoF) with the number of cycle of wear. Both coatings show similar trends at normal loads of 3.5 and 7 N. At 3.5 N, the CoF increases to 0.85 in the initial run-in period and stabilizes after around 250 cycles to 0.5 in the steady state regime. Similarly, at 7 N, the CoF increases to 0.85 in the initial run-in period, followed by a drop to the steady state regime with a CoF of 0.55. At 7 N normal loads, the drop to the steady state regime is intermittent for C-ZnNi and more gradual for D-ZnNi. This could be attributed to the difference in coating morphology and different velocity accommodation mechanisms (VAMs). At 12 N normal load, there are differences in the CoF between the coatings. For D-ZnNi, an increase of the CoF to 0.85 is observed in the run-in period, followed by a steady state regime at a CoF of 0.7. In contrast, with C-ZnNi, the CoF rises to 0.7 and stabilizes after around 100 cycles until the end of the test. The steady state CoF for C-ZnNi at 12 N is less stable than D-ZnNi and could be due to different VAMs.

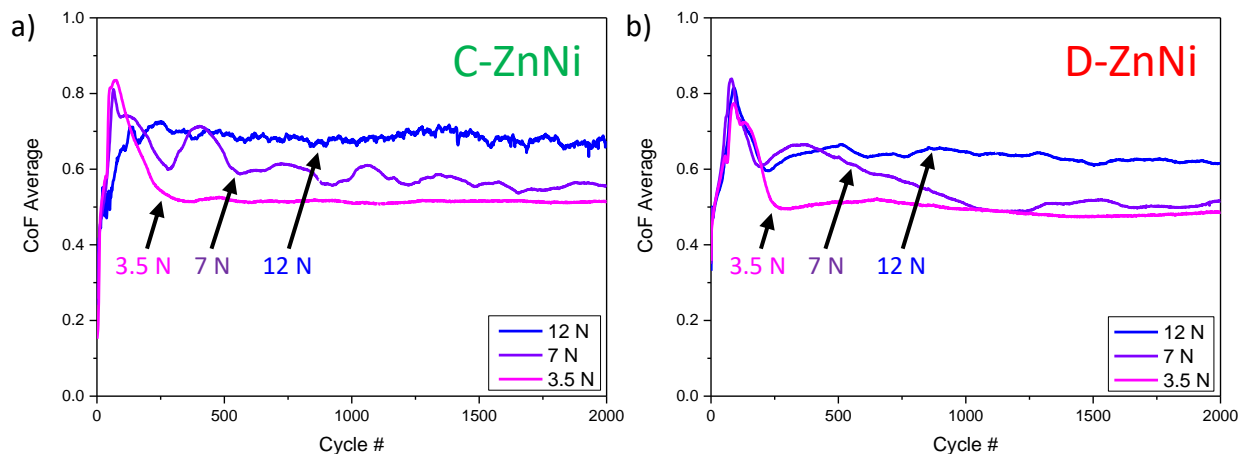


Figure 4. Average coefficient of friction evolution at 12, 7 and 3.5 N for a) C-ZnNi and b) D-ZnNi

Secondary electron images of the wear tracks are shown in Figure 5-6. Tests performed at normal loads of 3.5 and 7 N showed mild wear in both coatings, where increasing the normal load increased the severity. After 10 cycles, only asperity wear is observed and after 2000 cycles there is a more distinguishable wear track (Figure 5). However, the coating is still intact and unworn coating is observed within the wear tracks. Shear marks and plastic deformation are observed on the surfaces of the flattened asperities (Figure 7). For D-ZnNi, as the tests progress, the asperities appear to coalesce by closing the through coating thickness porosity (Figure 7).

Increasing the normal load to 12 N resulted in more severe wear in both coatings. With C-ZnNi, after 75 cycles, a clear wear track is observed with score lines running along the wear track. After 2000 cycles, deeper score lines and a wider wear track are observed. Score lines observed in this condition appears to be ploughed (Figure 8). With D-ZnNi, there is mild wear after 75 cycles. After 2000 cycles, a wider wear track and score lines through plastic deformation are observed. Shear marks and plastic deformation are observed on the surface of the wear track, similar to tests performed at lower normal loads. Although the wear track is wider, pockets of unworn coating are still observed in the wear track (Figure 9).

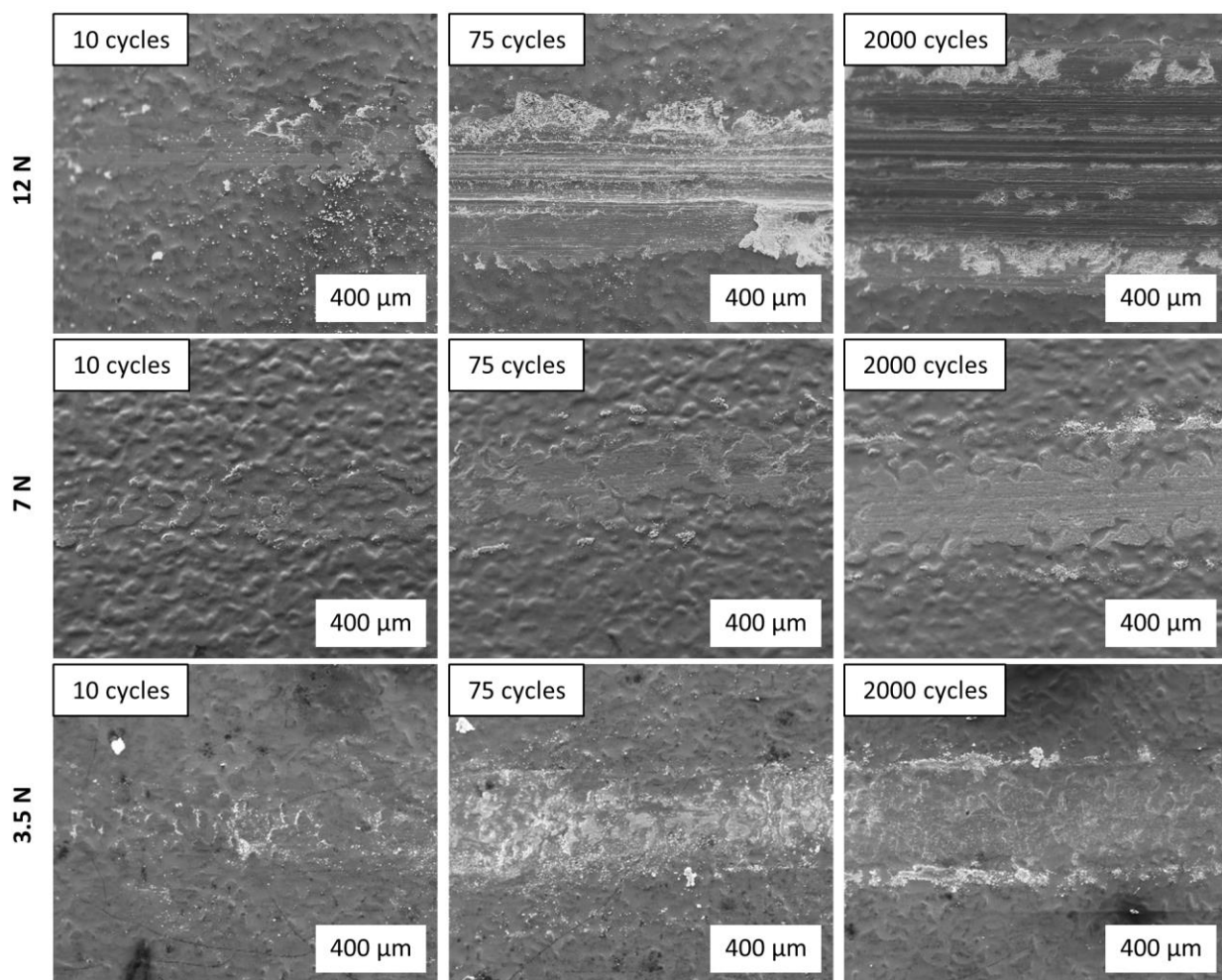


Figure 5. SEM images of wear tracks at 10, 75 and 2000 cycles under conditions 3.5, 7 and 12 N normal load for C-ZnNi. Sliding direction ↔

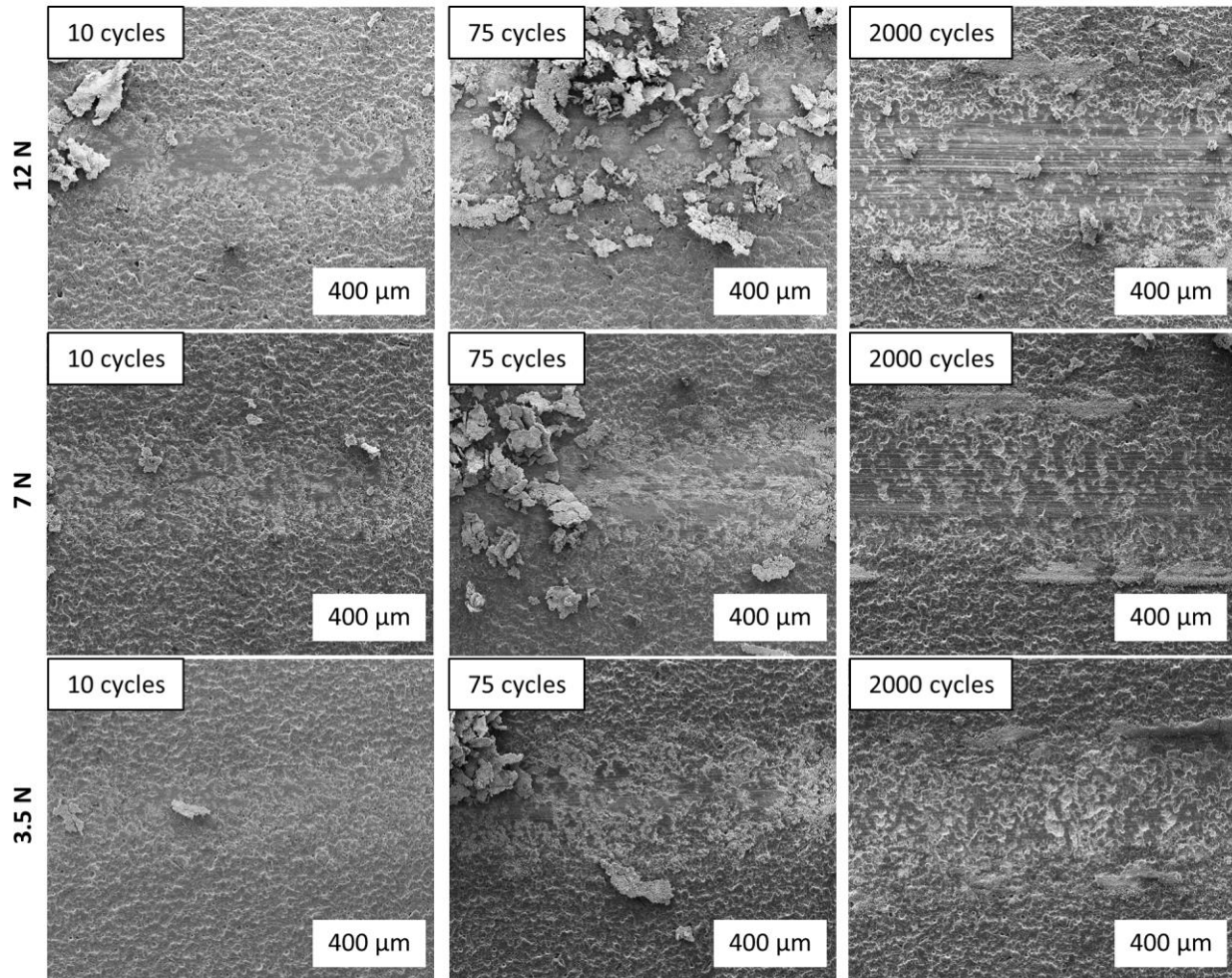


Figure 6. SEM images of wear tracks at 10, 75 and 2000 cycles under conditions 3.5, 7 and 12 N normal load for D-ZnNi. Sliding direction ↔

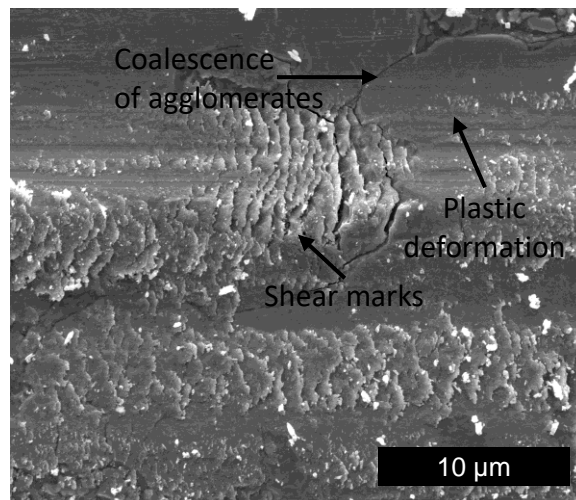


Figure 7. SEM image of D-ZnNi coating under 12 N load after 2000 cycles showing features on wear track

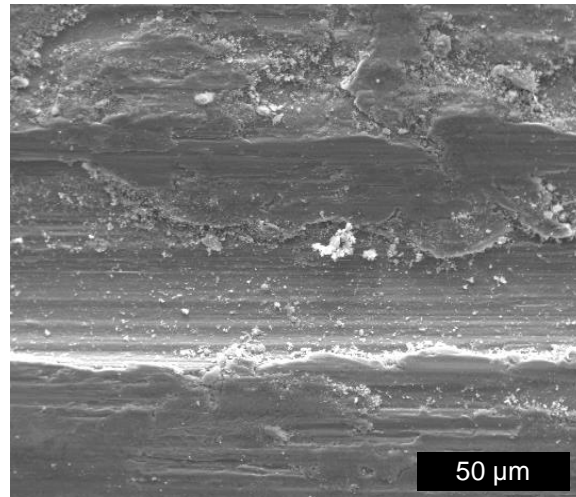


Figure 8. SEM image of C-ZnNi at 12 N normal load after 500 cycles of wear – ploughed feature

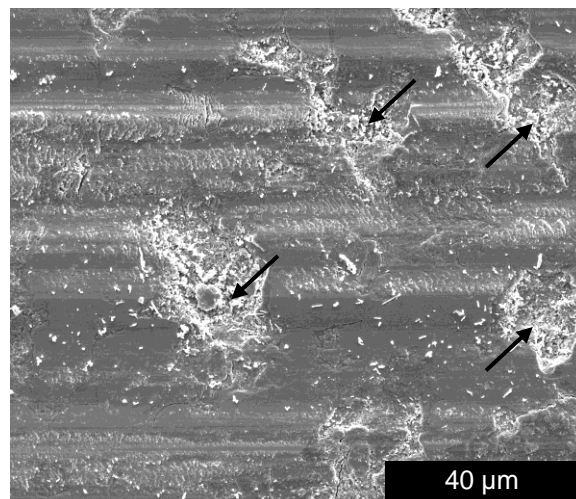


Figure 9. SEM image of wear track of D-ZnNi coating after 2000 cycles of wear under 12 N normal load with arrows showing pockets of coatings that have not been worn

3.4 Wear Rate

Wear volumes and wear rates are calculated for both coatings and are shown in Figure 10-11. The wear volume (Figure 10a) of C-ZnNi conducted at 12 N normal load condition increases throughout the test, while tests conducted at 3.5 and 7 N shows little increase in wear volume as the test progresses. This suggests that for tests conducted at lower normal loads, wear occurs mostly in the initial run in period, while for 12 N condition, wear occurs throughout the test and becomes more severe as the test progresses, especially between cycles 850 and 2000. A dependence of the wear volume on the normal load is observed for C-ZnNi coating, as increasing the normal load from 3.5 N to 7 N increases the wear volume slightly, while when the normal load is increased from 7 N to 12 N, a drastic increase in wear volume is observed, especially near the end

of the test. For C-ZnNi at 12 N between 850 to 2000 cycles, the depth of the wear track increased from less than 5 μm (less than the coating thickness) to around 20 μm (more than the coating thickness). This indicates the substrate contributed to part of the wear volume measured at 2000 cycles.

For the wear volume of D-ZnNi coatings (Figure 10b), higher wear volume is observed when compared to C-ZnNi under 3.5 and 7 N normal loads. However, increasing the normal load from 3.5 to 12 N did not change the wear volume significantly for D-ZnNi coatings. In comparison to C-ZnNi coating, there is little dependency of the wear volume to the normal load at the beginning of the test for D-ZnNi. This trend may be due to the morphological differences between the coatings. Near the end of the test, a slight dependency of the wear volume to the normal load is observed, as increasing the normal load increases the wear volume slightly.

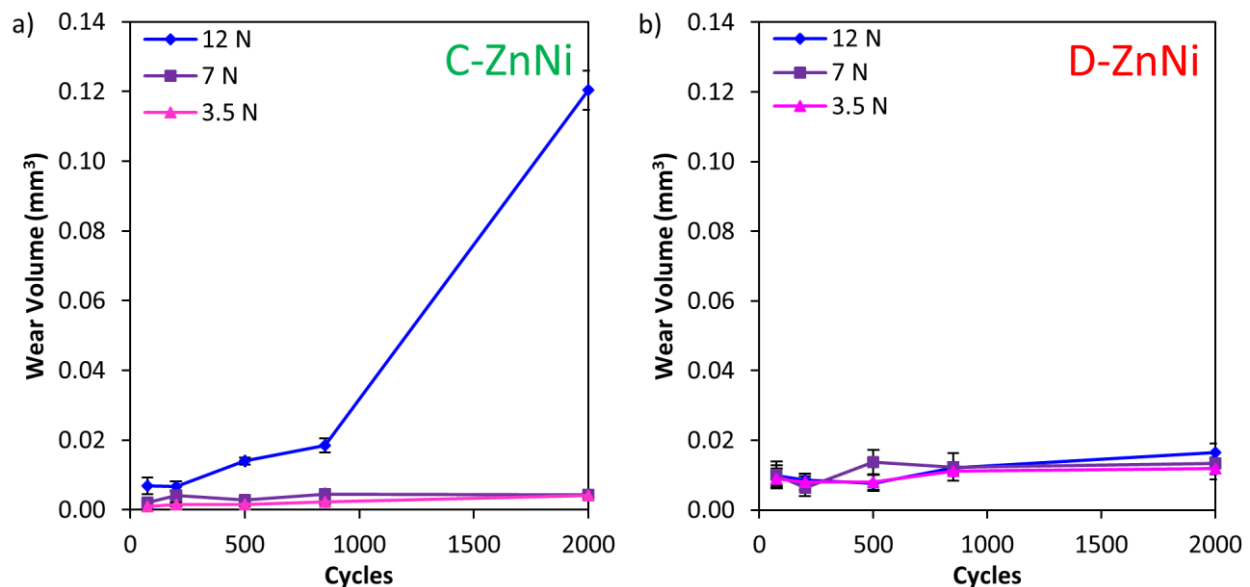


Figure 10. Wear volume comparison of 12, 7 and 3.5 N normal loads for a) C-ZnNi and b) D-ZnNi coatings

With regards to the wear rate (Figure 11a), for normal loads of 3.5 and 7 N, a decreasing wear rate is observed for C-ZnNi coatings, which coincides with the run-in period in the CoF evolution (Figure 4a), indicating most of the wear occurring during the run-in period where both the wear rate and CoF are high, before stabilizing to a low wear rate in the steady state regime. At 12 N normal load, a decreasing wear rate is also observed in the initial cycles. However, the wear rate is higher than the lower normal load and an increase in wear rate is observed after 850 cycles, indicating a large amount of the coating is removed from the wear tracks and is a combination of coating wear and

substrate wear. This trend agrees with the SEM images of the wear track morphologies where little wear is observed for tests performed at 3.5 and 7 N, while at 12 N, substantial wear occurred and the substrate is exposed.

A decreasing wear rate trend is also observed for D-ZnNi in all three normal load conditions (Figure 11b). Wear rates in the run-in period is high due to the flattening of asperities and formation of a transfer film at the initial cycles. Lower wear rates are observed at later cycles during the steady state regime. As opposed to C-ZnNi coatings, the wear rate decreases with an increasing normal load, which could be attributed to plastic deformation of the agglomerates resulting in closing of the porosity of the coating. The wear rates are also higher with D-ZnNi coatings.

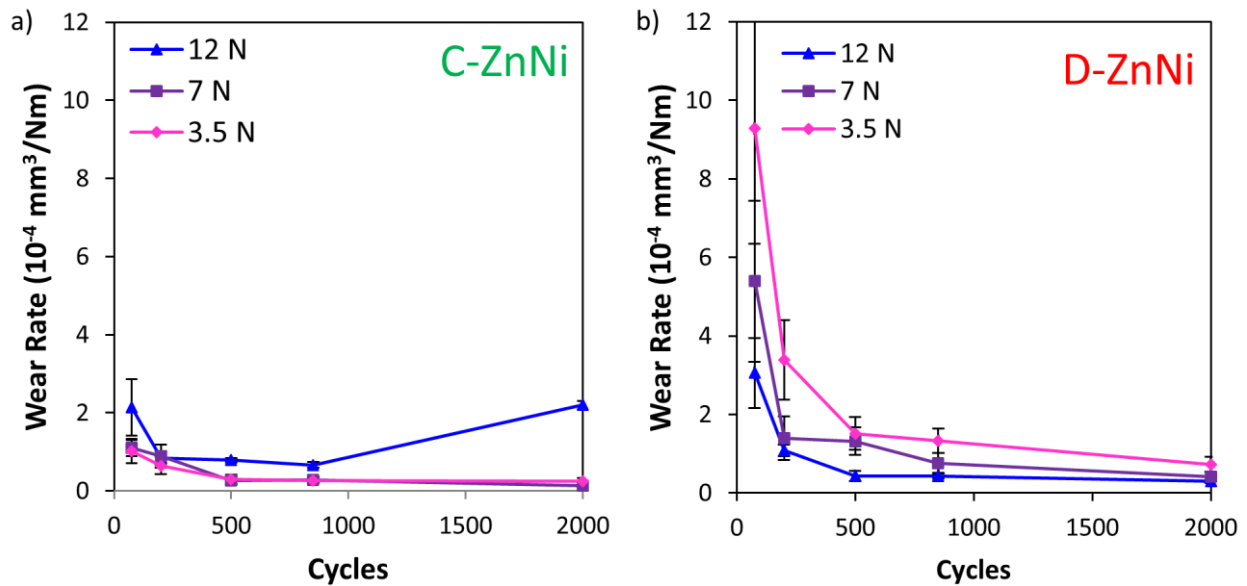


Figure 11. Wear rate comparison of 12, 7 and 3.5 N normal loads for a) C-ZnNi and b) D-ZnNi coatings

Another method of analyzing metallic wear is through the power law (Equation 2) proposed by Siniawski *et al.* [33]. This equation looks at wear through the wear rate, where $A(n)$ is the average wear rate, V_n is the average wear volume at n cycles, d is the sliding distance, A_1 is the wear rate at the first cycle, and β is a constant of the wear rate. By plotting the average wear rate, $\overline{A(n)} = V_n/d$ to the number of cycles, A_1 and β can be obtained.

$$\overline{A(n)} = \frac{V_n}{d} = A_1 n^\beta, \quad (\text{Eq 2})$$

Table 1. Siniawski's model parameter results

Coating	Load (N)	A_1 (mm ³ /m)	β	RMS
C-ZnNi	3.5	2.5×10^{-3}	-0.47	0.21
	7	1.5×10^{-2}	-0.67	0.27
	12*	1.5×10^{-2} *	-0.45 *	0.27 *
D-ZnNi	3.5	7.6×10^{-2}	-0.76	0.18
	7	6.5×10^{-2}	-0.72	0.30
	12	6.1×10^{-2}	-0.71	0.30

* Results from 2000 cycles are not used in calculations due to substrate wear.

From the results shown in Table 1, β is negative for both coatings at all 3 load conditions, which is normally observed for metal-metal contacts [33]. However, β is more negative for D-ZnNi than C-ZnNi. β is indicative of the time dependence of the wear rate and when $\beta = -1$, most of the wear is lost in a single cycle, whereas when $\beta = 0$, the wear rate is constant [33]. Therefore, as D-ZnNi is more negative than C-ZnNi, most of the wear occurs earlier in the tests than for C-ZnNi coatings. This is also indicated in the A_1 values, as the wear rate in the first cycle is much lower for C-ZnNi than D-ZnNi. It is also interesting to note that at normal loads of 3.5 N, the wear loss is lower than at normal loads of 7 and 12 N for C-ZnNi, while it is higher for D-ZnNi. This may be due to the morphological differences between the coatings, as for a smoother and fully dense coating such as C-ZnNi, a higher amount of energy is needed to initiate wear, than for a rougher and porous coating such as D-ZnNi [19]. The lowered A_1 at 7 and 12 N normal loads for D-ZnNi coatings could be due to smoothing of the coating through plastic deformation and coalescence of the asperities resulting in larger flattened areas (Figure 6 & 7).

3.5 Chemical analysis of wear track

Chemical changes on the surface of the wear tracks were characterized using Raman spectroscopy (Figure 12). Peaks corresponding to zinc oxide ($A_1(\text{LO})$, $A_1(\text{TO})$, $E_2(\text{high})$ and second order scattering bands of wurtzite [34-37]) were detected on the darker films and particles on the wear tracks in all cases. A high intensity and broad peak at the $A_1(\text{LO})$ band observed could be related to the crystallographic orientation and microstructure of the zinc oxide layer due to sliding [34, 35]. Through optical microscopy, higher ZnO film coverage was observed for the wear tracks obtained using lower normal loads compared to wear tracks from tests with higher normal loads, where the film is mostly broken up and partially removed. For D-ZnNi coatings, recesses of the unworn coating are present throughout the wear track which contained zinc oxide particles.

Patches of zinc oxide films were also detected on the surface of the wear track, although to a lesser degree as the load is increased.

In the case of C-ZnNi, at a low normal load, compact zinc oxide films are formed on the surface of the wear track. Raman mapping shows that the dark compact films correspond to zinc oxide (Figure 13). At 7 N normal load, the coating did not wear through after 2000 cycles, and patches of compact zinc oxide film were again observed on the surface, but to a lesser degree. Optical images of the wear tracks were taken at high and low friction during the intermittent steady state regime for C-ZnNi under 7 N load (Figure 14). Raman spectroscopy of the dark films again showed zinc oxide peaks for both cases. However, the zinc oxide films on the lower friction instances are more continuous and thicker than the zinc oxide films observed at the higher friction instances, which contained thinner zinc oxide films in the form of streaks. There is a competition between building up and wearing of the zinc oxide film, which may have influenced the intermittent behaviour observed for tests at 7 N loads on C-ZnNi coatings. At 12 N, after 2000 cycles, the coating has been worn through. Optical images of the wear track show a grayish film on the surface of the wear track, which through Raman spectroscopy, corresponded to iron oxide peaks [38, 39] and a mixed iron and zinc oxide peak at 652 cm^{-1} [34, 38, 39]. As the coating does not contain iron, iron from the zinc and iron oxide mixed layer may have originated from either the counterface, substrate or both.

Chemical analysis of the surface of the wear track was also performed through EDX at 12 N normal load to understand the differences between the two coatings. For D-ZnNi coatings, even after 2000 cycles of wear, iron content is minimal on the surface of the wear track. On the other hand, for C-ZnNi coatings, strong iron peaks are observed as early as 75 cycles of wear in the score line where the coating appears to be removed, although the profilometry data indicates less than $5\text{ }\mu\text{m}$ wear depth. This is also observed after 850 cycles of wear. After 2000 cycles of wear, strong iron peaks are observed throughout the coating, which may be due to substrate exposure or transfer material from the counterface. The depth of the wear track is also around $20\text{ }\mu\text{m}$, indicating possible substrate exposure and wear between 850 and 2000 cycles.

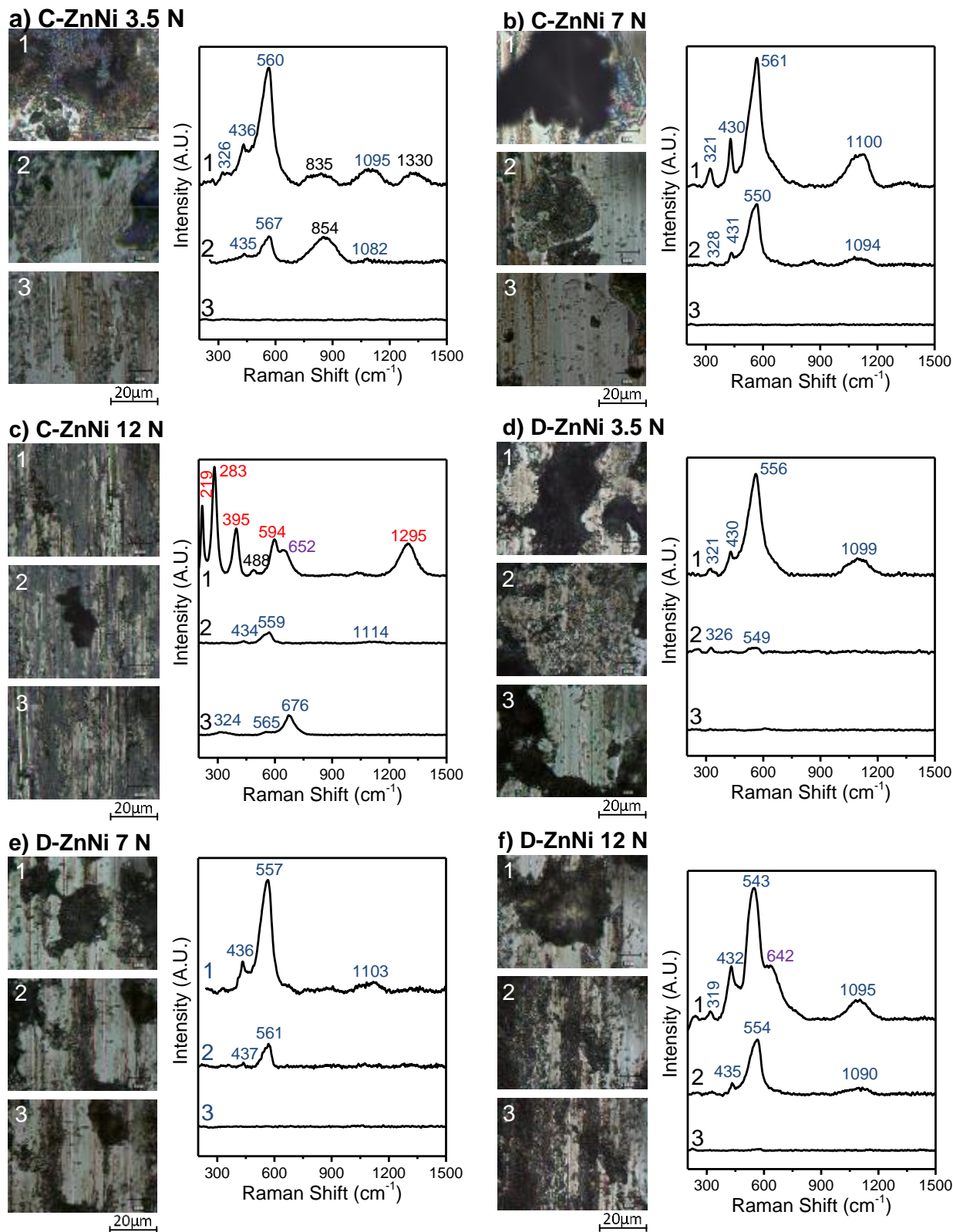


Figure 12. Raman Spectroscopy of wear tracks after 2000 cycles of wear for C-ZnNi (a-c) and D-ZnNi (d-f) coatings at 3.5, 7 and 12 N normal loads. ZnO [34-36], FeO [38, 39] and FeO + ZnO [34, 38, 39] peaks.

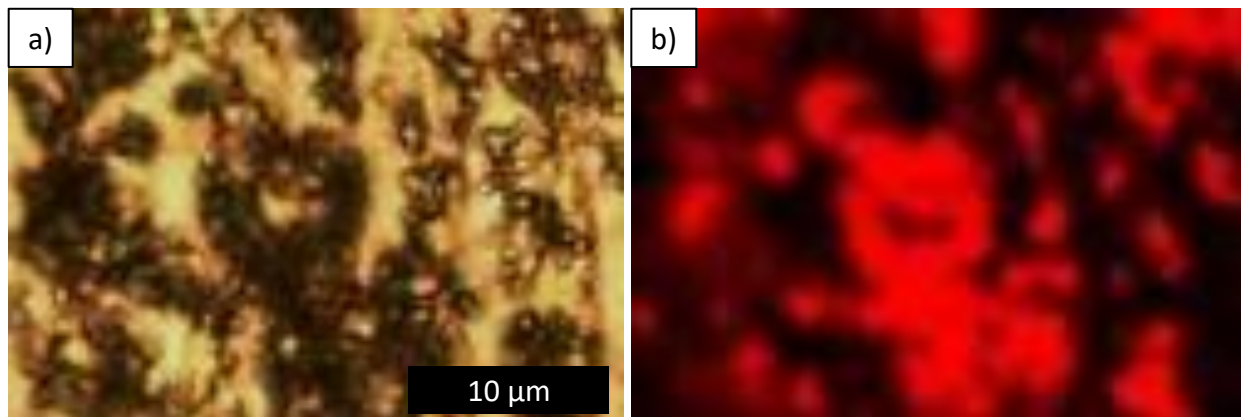


Figure 13. Raman maps of C-ZnNi coating under 3.5 N normal load a) optical image and b) Raman map for presence of ZnO ($490-600\text{ cm}^{-1}$)

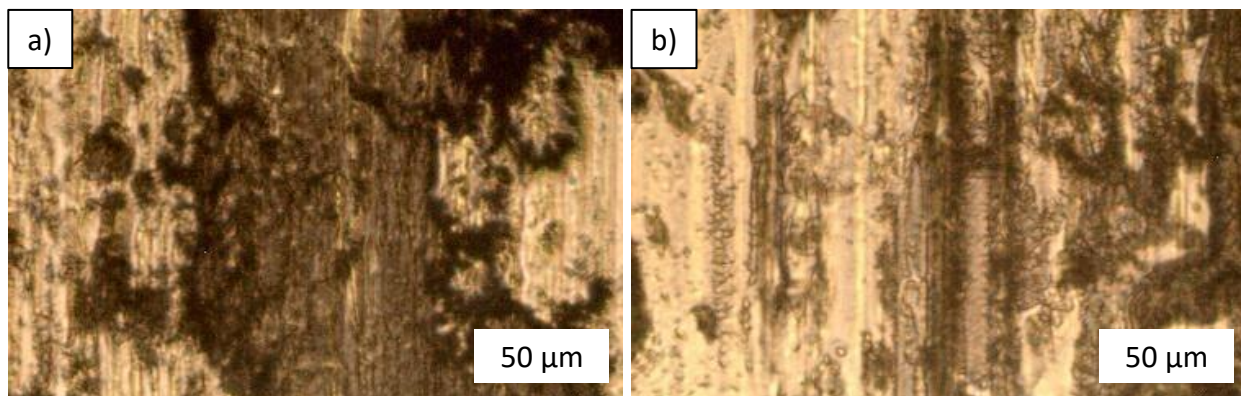


Figure 14. Optical images of wear tracks of C-ZnNi coating under 7 N normal load at a) low intermittent friction and b) high intermittent friction

3.6 Counterface

Secondary electron images of the transfer film are shown in Figure 15. In all cases, coating material was transferred to the counterface as EDX on the transfer films showed Zn and Ni. The size of the contact area corresponds to the width of the wear tracks. For C-ZnNi coatings, a small transfer film is observed at tests performed at 3.5 and 7 N tests, whereas for tests performed at 12 N, a large area of contact is observed. For D-ZnNi coating, a similar sized contact area is observed at all three normal load conditions. Although the size of the contact area for D-ZnNi coating is larger than the contact area of C-ZnNi coatings at 3.5 and 7 N conditions, at 12 N the contact area remains similar size to the lower normal load conditions.

A large amount of ball wear is observed at the center of the contact of tests performed under 12 N loads for C-ZnNi coatings. To calculate the volume lost at the end

of the tests, 3D profiles of the transfer film are obtained using white light interferometry. With both coatings, increasing the load increased the wear volume as shown in Table 2, while the height of the spherical cap remained similar with the exception of C-ZnNi under 12 N normal load (around 0.8 μm for C-ZnNi coatings conducted at 3.5 and 7 N normal loads, and 2.5-3.5 μm for D-ZnNi coatings conducted at 3.5, 7 and 12 N normal loads). This may be due to increase in contact area because of increased normal loads, resulting in an increase in wear volume, while the height of the spherical caps remained similar. A larger wear volume and spherical cap height are also observed in D-ZnNi coatings, which could be due to the rougher initial surface morphology of the coating itself or a slightly higher coating hardness of D-ZnNi coatings. For C-ZnNi coatings under 12 N normal loads, substantial of material from the counterface is removed, and the wear volume and spherical cap height (around 6 μm) is the highest among the different test conditions. Substantial material loss from the counterface is due to abrasive particles in the wear track. As humidity is high on the test performed, the formation of a prow, observed in a previous study [40], is hindered. Thus, the counterface and abrasive particles are not separated. This caused substantial material loss on the counterface at 12 N. This in contrast, is not observed in D-ZnNi at 12 N due to fewer wear particles because of the lower amount of wear, and particles falling into the recesses of the coating due to its morphology.

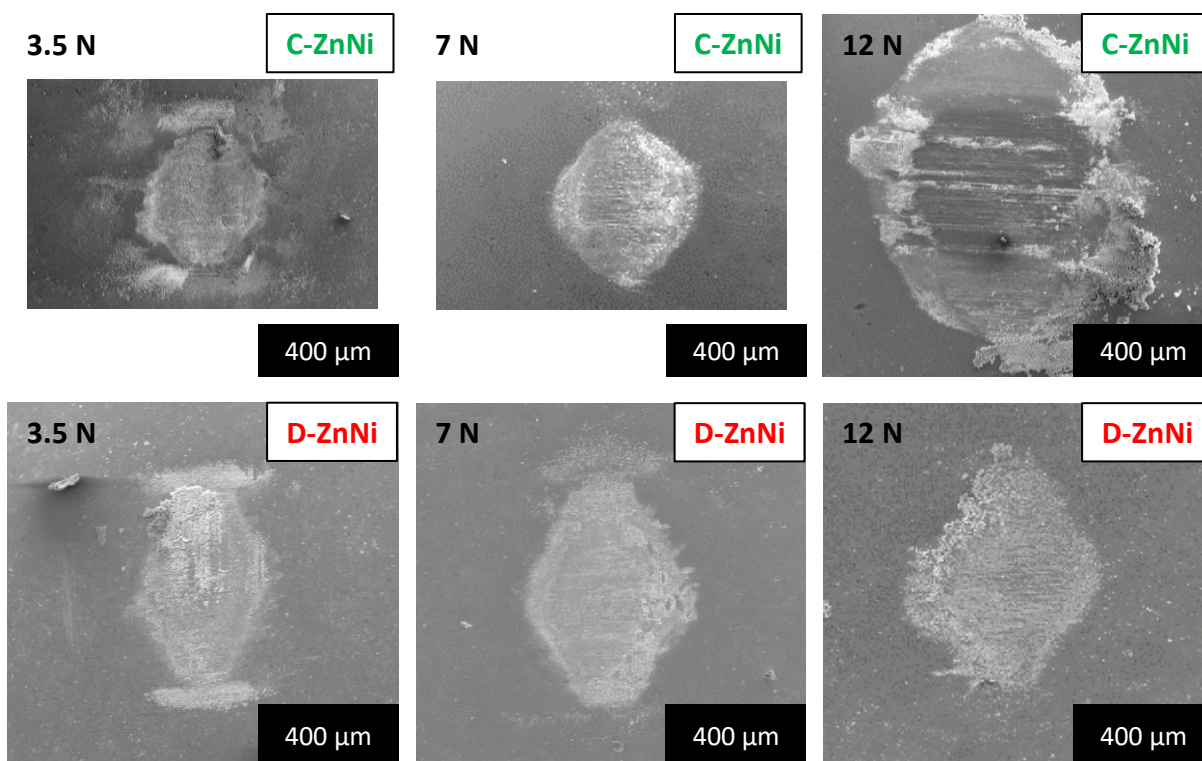


Figure 15. Transfer film after 2000 cycles for C-ZnNi and D-ZnNi coatings under 3.5, 7, and 12 N normal load (\leftrightarrow sliding direction)

Table 2. Counterface wear volume

	CF wear volume (mm ³)	
	C-ZnNi	D-ZnNi
3.5 N	1.9 x 10 ⁻⁵	4.1 x 10 ⁻⁵
7 N	2.0 x 10 ⁻⁵	10.8 x 10 ⁻⁵
12 N	58.0 x 10 ⁻⁵	17.9 x 10 ⁻⁵

4. Discussion

4.1 Effect of normal load and coating morphology on the CoF

In all normal load conditions, except for C-ZnNi under 12 N normal load, an increase of the average CoF to around 0.8 during the run-in period followed by a steady state regime with a lower average CoF after around 200 cycles is observed for both coatings (Figure 4). During the run-in period, an increase in the CoF is observed due to the formation of a transfer film and tribofilm, through flattening and wearing of the asperities. During the steady state regime, a general increase in normal load (consequently increase in the initial Hertzian contact stress (IHCS)) corresponded to an increase in CoF for both coatings. Increasing the IHCS increases the contact area [22]. This is reflected in the SEM images (Figure 5-6) where the worn asperity size in the run-in period and the wear track width in the steady state period is increased. The exception observed in C-ZnNi coating under 12 N normal load, where the initial increase of the CoF is not observed in the run-in period and the CoF is less stable than D-ZnNi in the steady state regime. The difference is due to a different wear mechanism, as adhesion tests have shown cracks and spallation occurring for C-ZnNi coating at high loads. Also, score lines and substantial material removal after 75 cycles indicate much more wear occurring at the earlier stage of the test performed with 12 N normal load. Flattening of the asperity also occurs faster and earlier during the test due to increased adhesion caused by the oxide film break down at high loads, which may be why the initial increase in the CoF is not observed.

During the steady state regime, an intermittent CoF is observed for tests conducted at 7 N. This could be due to oxide break down and reformation, as there are areas in the wear track where the oxide film is absent. Furthermore, increasing the load generally resulted in an increased CoF in the steady state regime. This is due to the oxide film break down as the load is increased and the larger contact area due to faster flattening of the asperities or closing of pores in the case of D-ZnNi, which may contribute to the higher steady state friction observed. A less stable CoF is also observed for C-ZnNi at 12 N. This is due to the large amount of wear particles and the steel substrate being

exposed, which contributes to the adhesion between the counterface and wear track, and the higher and less stable CoF when compared with D-ZnNi.

4.2 Effect of normal load and coating morphology on the wear

Although the effects of normal load and coating morphology on the friction behaviour are similar, wear behaviour, on the other hand, differed (Figure 10-11). At low normal load (3.5 and 7 N) a lower wear rate and wear volume is observed in C-ZnNi coatings than in D-ZnNi coatings. However, at 12 N normal load, higher wear rate and wear volume are observed for C-ZnNi coatings. Morphological differences between the coatings contribute to the differences observed. Both coatings have through coating thickness defects. However, C-ZnNi is a smooth and dense coating with vertical cracks, whereas D-ZnNi is a rough coating with through-thickness porosity and cracks along the platelet agglomerates. At low normal loads, a higher wear rate and wear volume are observed for D-ZnNi as defects along the agglomerates allow for easier removal of the coating, resulting in a higher wear rate and wear volume. Previous fretting wear tests done with the same coatings shows more severe wear in D-ZnNi coatings as it was easier to remove coating material when sliding occurs [15]. The surface roughness affects the wear at the initial stages and an increase in surface roughness is associated with an increase in wear rate. At high normal load (12 N), an increasing wear rate and high wear volume are observed for C-ZnNi coatings, while the wear rates and wear volumes for D-ZnNi coatings at this condition remains similar to tests conducted at lower normal loads. The higher wear of the counterface and wear track observed for C-ZnNi at 12 N is due to the combination of large amount of particles formation because of wear and steel on steel contact between the counterface and wear track.

The high amount of wear particles produced at 12 N load for C-ZnNi coating is largely due to the lack of ZnO film present in the wear track. During high loads, the ZnO film is broken down and removed from the wear track, which results in adhesive wear. The difference between C-ZnNi and D-ZnNi lies in their different morphologies, as the columnar structure of D-ZnNi allows a degree of compliance through elastic and plastic deformation of those columns [41, 42]. In contrast, C-ZnNi coatings are likely to form cracks in order to accommodate the motion [15, 41], which facilitates the removal of the ZnO layer and the generation of wear particles that are ejected from the wear track and thus causes high wear.

4.3 Effect of normal load and coating morphology on the wear and velocity accommodation mechanisms

Oxide formation aids in stabilizing the CoF and lowering the wear rate for these coatings at the low normal load conditions, as the oxide layer acts as a lubricant between the counterface and the coating in many cases [21, 43]. Nanocrystalline ZnO coatings

have been reported to aid in reducing the CoF and wear rate [35, 44, 45]. However, when the normal load increases, the oxide layer begins to break down, as observed through the combination of optical images and Raman (Figure 12), and the velocity accommodation becomes adhesive in nature, which could occur where there is an absence of the oxide [21, 40, 43]. This mechanism is shown in Figure 16, where when a low normal load is used, such as 3.5 and 7 N, the tips of the asperities are flattened and a thin oxide layer is formed for both coatings during the run-in period. The velocity is accommodated through shearing the oxide layer (Figure 16), which resulted in stable CoFs and low wear rates in both cases.

When the normal load is increased, such as to 12 N, the oxide layer is broken down due to the high forces and is partially removed from the contact. This is exemplified in Figure 12, where at high loads there is less ZnO film coverage in the wear track. The lower ZnO film coverage results in adhesion between the coating and counterface and more severe wear to occur (Figure 16). Since C-ZnNi is a denser coating and D-ZnNi has more of a columnar structure, it is easier to deform the columnar structure found in D-ZnNi to accommodate the motion than the fully dense C-ZnNi. Consequently, for C-ZnNi severe wear is observed in the coating and counterface (Figure 16a), and a higher CoF is observed. In contrast for D-ZnNi, although the CoF and wear are increased, it is less severe, as the asperities can deform plastically and elastically to accommodate the motion [41, 42] (Figure 16b). This was also observed in a previous study from the authors using the same coatings [15], where during high load fretting tests, cracks formed in the contact area of C-ZnNi coatings, whereas for D-ZnNi coatings, asperities were plastically deformed in the stick regime, which shows that when there are high adhesion due to high load, C-ZnNi was more likely to debond than D-ZnNi coatings. This can also be attributed to the different residual stresses of the coatings as the biaxial residual stresses are tensile for C-ZnNi but compressive for D-ZnNi coatings. Tensile residual stresses can lead to debonding of the coating when external stresses are applied to the coating.

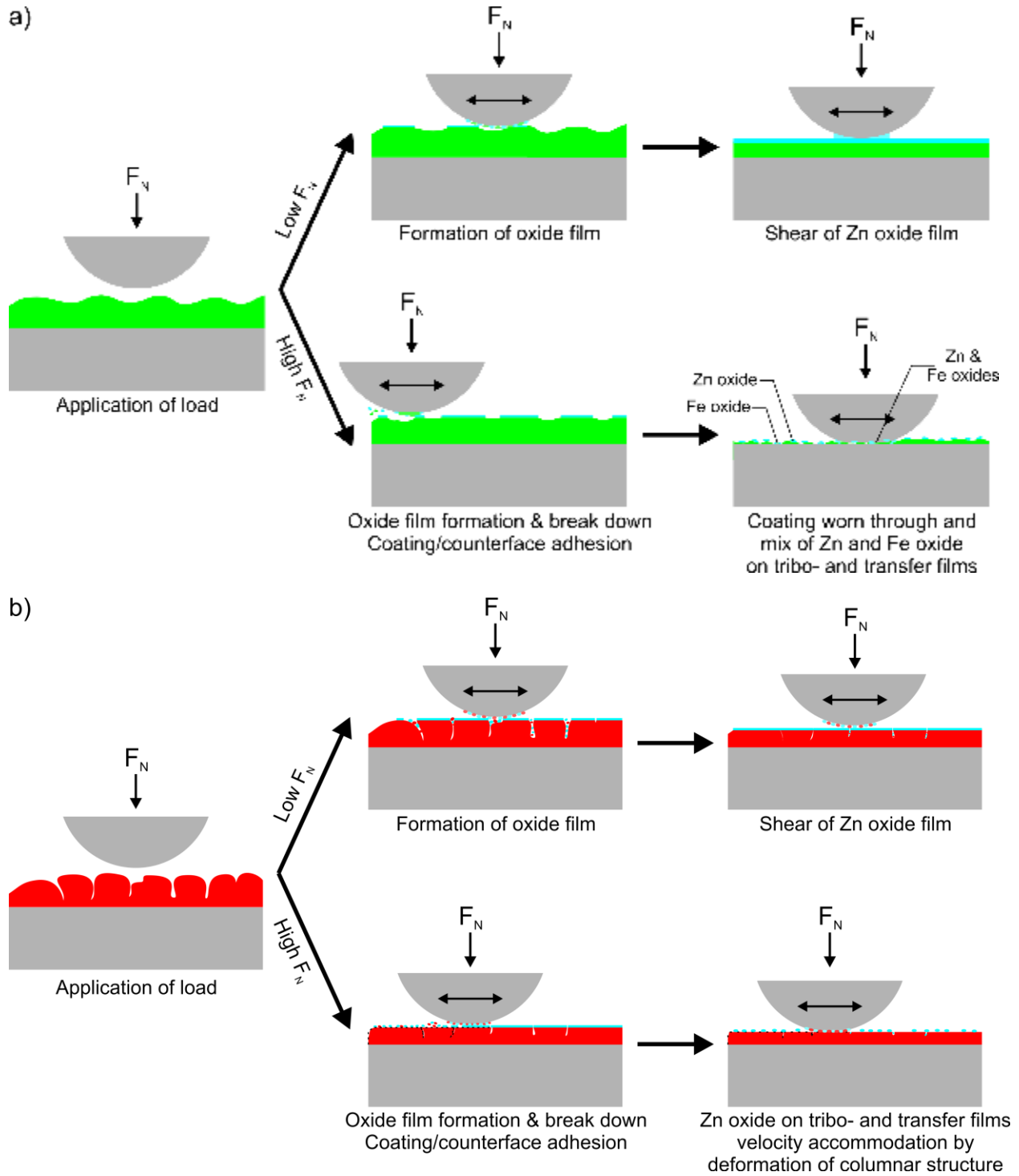


Figure 16. Schematic of wear and velocity accommodation mechanisms for a) C-ZnNi and b) D-ZnNi coatings at high (12 N) and low (3.5 and 7 N) normal loads

4.4 Applications

Zn-Ni coating is primarily used as a replacement for Cd coatings in the aerospace industry. It is, therefore, useful to discuss these coatings in comparison with Cd coatings. Cadmium coatings are a softer coating than Zn-Ni coatings. Thus, it is not surprising that the CoF of Cd is lower than Zn-Ni due to the lower stress needed to shear Cd given the same sliding parameters and conditions [46, 47]. However, the wear of Cd coatings is also higher than Zn-Ni coatings due to its lower hardness [46, 47]. Thus, there is merit in replacing Cd with Zn-Ni coatings.

The formation of ZnO is important for the lubricity of Zn-Ni coating, but changes in the sliding parameter and conditions, such as the change in humidity [40] or change in normal load, can favour or impede the formation of ZnO and affect the performance of these coatings. Lower humidity impedes the formation of ZnO [40], while a higher load results in a break down of the ZnO film. It is therefore important to consider the environment and application (high or low humidity and forces) when selecting the coatings, such as higher humidity conditions to favour the formation of nanocrystalline ZnO, or a rougher and more porous coating for higher load application and a smoother and denser coating for lower loads conditions for the longevity of the coatings during tribological situations.

5. Conclusion

The effects of normal load and coating morphology on the tribological behaviour are studied. Similar friction behaviour trends are observed in both coatings at all contact conditions except for C-ZnNi coatings at 12 N normal load due to the difference of wear mechanisms. The increase of the normal load resulted in an increase of CoF in the steady state in both coatings. Wear behaviour between the coatings is different due to the difference in coating morphology. At 3.5 and 7 N, wear rate and wear volume of D-ZnNi coatings are higher than C-ZnNi coatings due to higher coating roughness and morphology of the coating defects in D-ZnNi. At 12 N, more severe wear occurred in C-ZnNi coatings due to debonding of the coating. An increase in initial Hertzian contact stress resulted in the increase in wear rate and wear volume for C-ZnNi coatings, while a decrease in wear rate and little change in wear volume is observed for D-ZnNi. This suggests that wear behaviour of C-ZnNi coatings are more sensitive to the change in IHCS than D-ZnNi due to the morphological and residual stress differences of the coatings.

6. Acknowledgement

The authors would like to thank Salim Brahimy for his continual support and inputs throughout the experiments. We would also like to thank Natural Science and Engineering Research Center (NSERC), Boeing Canada, Pratt & Whitney Canada, Héroux Devtek, Canadian Fastener Institute and Messier-Bugatti-Dowty for their financial support. We would also like to thank Boeing, Coventya and Dipsol Inc. for providing specimens.

7. References

- [1] G.D. Wilcox, D.R. Gabe, Electrodeposited zinc alloy coatings, *Corrosion Science*, 35 (1993) 1251-1258.
- [2] Ministry of Defence, Guidance to the Use of Cadmium Alternatives in the Protective Coating of Defence Equipment, Defence Standard 03-36 Crown, Glasgow, 2010.
- [3] K.R. Sriraman, H.W. Strauss, S. Brahimy, R.R. Chromik, J.A. Szpunar, J.H. Osborne, S. Yue, Tribological behavior of electrodeposited Zn, Zn-Ni, Cd and Cd-Ti coatings on low carbon steel substrates, *Tribology International*, 56 (2012) 107-120.
- [4] K.R. Baldwin, C.J.E. Smith, Advances in replacements for cadmium plating in aerospace applications, *Transactions of the Institute of Metal Finishing*, 74 (1996) 202-209.
- [5] M. Bielawski, Alternative technologies and coatings for electroplated cadmium and hard chromium, *Canadian Aeronautics and Space Journal*, 56 (2010) 67-80.
- [6] Cadmium REACH Consortium, Cadmium REACH, Brussels.
- [7] K. Legg, Cadmium Replacement Options Rowan Technology Group, 2003.
- [8] K.R. Sriraman, S. Brahimy, J.A. Szpunar, J.H. Osborne, S. Yue, Characterization of corrosion resistance of electrodeposited Zn-Ni, Zn and Cd coatings, *Electrochimica Acta*, 105 (2013) 314-323.
- [9] T.V. Byk, T.V. Gaevskaia, L.S. Tsybulskaya, Effect of electrodeposition conditions on the composition, microstructure, and corrosion resistance of Zn-Ni alloy coatings, *Surface and Coatings Technology*, 202 (2008) 5817-5823.
- [10] K.R. Sriraman, S. Brahimy, J.A. Szpunar, J.H. Osborne, S. Yue, Tribocorrosion behavior of Zn, Zn-Ni, Cd and Cd-Ti electrodeposited on low carbon steel substrates, *Surface and Coatings Technology*, 224 (2013) 126-137.
- [11] J.A. Bates, Comparison of alkaline Zn-Ni & acid Zn-Ni as a replacement coating for cadmium, *Plating and Surface Finishing*, 81 (1994) 36-40.

This is a post-peer-review, pre-copyedit version of an article published in *Wear*.
DOI:10.1016/j.wear.2017.12.018

[12] A. Conde, M.A. Arenas, J.J. de Damborenea, Electrodeposition of Zn-Ni coatings as Cd replacement for corrosion protection of high strength steel, *Corrosion Science*, 53 (2011) 1489-1497.

[13] H. Bruet, J.P. Bonino, A. Rousset, M.E. Chauveau, Structure of zinc-nickel alloy electrodeposits, *Journal of Materials Science*, 34 (1999) 881-886.

[14] S. Ghaziof, W. Gao, Electrodeposition of single gamma phased Zn-Ni alloy coatings from additive-free acidic bath, *Applied Surface Science*, 311 (2014) 635-642.

[15] L. Lee, É. Régis, S. Descartes, R.R. Chromik, Fretting wear behavior of Zn–Ni alloy coatings, *Wear*, 330–331 (2015) 112-121.

[16] C.N. Panagopoulos, K.G. Georgarakis, P.E. Agathocleous, Sliding wear behaviour of zinc-nickel alloy electrodeposits, *Tribology International*, 36 (2003) 619-623.

[17] S. Jahanmir, N.P. Suh, Surface topography and integrity effects on sliding wear, *Wear*, 44 (1977) 87-99.

[18] B. Bhushan, Nanotribology: Friction, wear and lubrication at the atomic scale, *Nature*, 374 (1995) 607-616.

[19] K.J. Kubiak, T.W. Liskiewicz, T.G. Mathia, Surface morphology in engineering applications: influence of roughness on sliding and wear in dry fretting, *Tribology International*, 44 (2011) 1427-1432.

[20] A. Riyadh, A. Khairil Rafezi, Y. Al-Douri, Evaluate the effects of various surface roughness on the tribological characteristics under dry and lubricated conditions for Al-Si alloy, *Journal of Surface Engineered Materials and Advanced Technology*, 2012 (2012).

[21] F.P. Bowden, D. Tabor, *The friction and lubrication of solids*, Clarendon Press ; Oxford University Press, Oxford; New York, 2001.

[22] F. Bowden, D. Tabor, Friction, lubrication and wear: a survey of work during the last decade, *British Journal of Applied Physics*, 17 (1966) 1521.

[23] D. Rigney, J. Hirth, Plastic deformation and sliding friction of metals, *Wear*, 53 (1979) 345-370.

[24] B. Bhushan, *Introduction to tribology*, John Wiley & Sons Inc., New York, 2013.

[25] L. Thiery, L. Moui, J.J. Duprat, *Performa 280.5*, Coventya, UK, 2004.

[26] Coventya, *Protection : technical sheets and documentation*, Coventya, France, 2013.

[27] B.B. He, *Two-dimensional x-ray diffraction*, Wiley, Hoboken, N.J., 2009.

This is a post-peer-review, pre-copyedit version of an article published in *Wear*.
DOI:10.1016/j.wear.2017.12.018

[28] J.F. Archard, W. Hirst, The Wear of Metals under Unlubricated Conditions, *Proceedings of the Royal Society of London. Series A, Mathematical and Physical Sciences*, 236 (1956) 397-410.

[29] C.S. Lin, H.B. Lee, S.H. Hsieh, Microstructure and formability of ZnNi alloy electrodeposited sheet steel, *Metallurgical and Materials Transactions A: Physical Metallurgy and Materials Science*, 31 (2000) 475-485.

[30] T. Sasaki, Y. Hirose, Residual stress distribution in electroplated Zn-Ni alloy layer determined by X-ray diffraction, *Thin solid films*, 253 (1994) 356-361.

[31] S.J. Bull, Failure mode maps in the thin film scratch adhesion test, *Tribology International*, 30 (1997) 491-498.

[32] S.J. Bull, E.G. Berasetegui, An overview of the potential of quantitative coating adhesion measurement by scratch testing, *Tribology International*, 39 (2006) 99-114.

[33] M.T. Siniawski, S.J. Harris, Q. Wang, A universal wear law for abrasion, *Wear*, 262 (2007) 883-888.

[34] K.R. Sriraman, P. Manimunda, R.R. Chromik, S. Yue, Effect of crystallographic orientation on the tribological behavior of electrodeposited Zn coatings, *RSC Advances*, 6 (2016) 17360-17372.

[35] J.S. Zabinski, J. Corneille, S.V. Prasad, N.T. McDevitt, J.B. Bultman, Lubricious zinc oxide films: Synthesis, characterization and tribological behaviour, *Journal of Materials Science*, 32 (1997) 5313-5319.

[36] T.C. Damen, S.P.S. Porto, B. Tell, Raman effect in zinc oxide, *Physical Review*, 142 (1966) 570-574.

[37] K.A. Alim, V.A. Fonoberov, M. Shamsa, A.A. Balandin, Micro-Raman investigation of optical phonons in ZnO nanocrystals, *Journal of Applied Physics*, 97 (2005).

[38] S.J. Oh, D.C. Cook, H.E. Townsend, Characterization of Iron Oxides Commonly Formed as Corrosion Products on Steel, *Hyperfine Interactions*, 112 59-66.

[39] S.H. Shim, T.S. Duffy, Raman spectroscopy of Fe₂O₃ to 62 GPa, *American Mineralogist*, 87 (2002) 318-326.

[40] L. Lee, P. Behera, K.R. Sriraman, R.R. Chromik, Effects of humidity on the sliding wear properties of Zn-Ni alloy coatings, *RSC Advances*, 7 (2017) 22662-22671.

[41] Y. Berthier, L. Vincent, M. Godet, Velocity accommodation in fretting, *Wear*, 125 (1988) 25-38.

[42] R.B. Waterhouse, *Fretting Corrosion*, Pergamon Press, Oxford; New York, 1972.

[43] J.K. Lancaster, A review of the influence of environmental humidity and water on friction, lubrication and wear, *Tribology International*, 23 (1990) 371-389.

This is a post-peer-review, pre-copyedit version of an article published in *Wear*.
DOI:10.1016/j.wear.2017.12.018

[44] S.V. Prasad, J.S. Zabinski, Tribological behavior of nanocrystalline zinc oxide films, *Wear*, 203–204 (1997) 498-506.

[45] J. Zhang, J. Zheng, Surfactant inducing phase change of ZnO nanorods to low friction, *Tribology Letters*, 49 (2013) 77-83.

[46] P. Behera, K.R. Sriraman, R.R. Chromik, S. Yue, Combining in situ tribometry and triboscopy to understand third body behavior of a Cd coating, McGill University, 2016.

[47] L. Lee, Sliding wear and fretting behaviour of electrodeposited γ -phase zinc-nickel coatings as a replacement for electrodeposited cadmium coatings, Department of Mining and Materials Engineering, McGill University, Montreal, Canada, 2017.